JOURNAL OF MATERIALS SCIENCE 13 (1978) 2197–2204

The fracture energy of hybrid carbon and glass fibre composites

J. N. KIRK*, M. MUNRO†, P. W. R. BEAUMONT
Department of Engineering, University of Cambridge, Trumpington Street, Cambridge, UK

The fracture energy of a model carbon fibre/glass fibre/epoxy resin hybrid composite system has been evaluated as a function of the carbon fibre/glass fibre ratio. Work of fracture measurements were less than a rule of mixtures prediction and a pronounced negative synergistic effect was observed at high carbon fibre and high glass fibre contents. Fibre debonded lengths and fibre pull-out lengths for the carbon and glass fibres were accurately measured using a projection microscope technique. Models of microscopic fracture behaviour, together with these measurements, were successful in quantitatively describing the observed fracture behaviour of the hybrid fibrous composites. It was found that post-debond friction energy provided a major contribution to the fracture energy of the glass fibres. The post debond sliding mechanism was also shown to be primarily responsible for the non-linear behaviour of the work of fracture of the hybrid composite.

1. Introduction

Fracture mechanisms at the microscopic level, in fibre strengthened brittle materials, can combine to give different kinds of macroscopic fracture behaviour [1]. Carbon fibre reinforced epoxy resin composites (CFRP), for instance, have a fracture toughness which is derived primarily from the frictional work to extract broken fibres out of a cracked matrix [2], while the fracture toughness of glass fibre reinforced epoxy resin composites (GRP) originates from the dissipation of energy in fibre–matrix debonding [3] and post-debond fibre sliding processes [4, 5]. It is logical to assume, therefore, that the combination of carbon fibres and glass fibres in the same matrix will produce a fibrous composite which processes some of the microfracture characteristics of the two individual composite systems.

Whether or not a hybrid fibrous composite has a fracture toughness that can be predicted by assuming a rule of mixtures relationship between the works of fracture of CFRP and GRP is not clear; on the one hand, Chamis *et al.* [6] imply that for carbon fibre/glass fibre hybrid composites the impact energy may be increased above that which is predicted by a mixtures' equation, while on the other, Harris and Bunsell [7] found that the impact energy of notched specimens made from carbon fibre/glass fibre hybrids followed the mixture rule, even though the work of fracture of their unnotched samples fell below such a prediction.

In this study detailed fracture experiments have been undertaken on model carbon fibre/glass fibre/epoxy resin composites for two principal reasons; first, to establish in a systematic way whether combining two dissimilar fibres in a common matrix produces a hybrid composite with a fracture toughness that can be predicted accurately using a rule of mixtures' equation, or whether synergistic effects can occur because of some interaction between the two different fibres; and second, to see whether the fracture energy of such hybrids can be estimated using existing fracture models for brittle fibrous composites. Previous studies [7–12] have made this com-

*Presently with Sheffield Laboratories, British Steel Corporation, Rotherham, UK.
†Presently with Department of Mechanical Engineering, University of Ottawa, Ottawa, Canada.

TABLE I Fibre and matrix properties

Material	No. of fibres per tow	Fibre diameter ($\times 10^{-6}$ m)	Tensile strength ($GN\,m^{-2}$)	Young's modulus ($GN\,m^{-2}$)	Calculated failure strain ϵ
Carbon fibre Type II	5000	8	2.40	240	0.010
Glass fibre Type E	1600	13	1.65	70	0.023
Epoxy resin CY219 + HY219	–	–	0.06	2.5	0.024

parison difficult for three main reasons: (1) there was a large amount of scatter in the experimental data due to differences in microstructure from specimen to specimen; (2) only a small number of different fibre combinations was examined and (3) the fibre–matrix debonded and fibre pull-out lengths could not be precisely measured.

In the present work an attempt has been made to overcome these difficulties by fabricating reproducible model specimens from single layer, unidirectional fibre hybrid tapes. A total of ten carbon fibre/glass fibre ratios were used and the choice of a transparent epoxy resin matrix permitted easy recognition and measurement of fibre debonded zones. A specimen was designed to ensure that all of the fibres failed in tension (rather than in both tension and compression as generally occurs in three-point bend tests) and that fibre pull-out lengths could be more accurately measured than in earlier studies.

2. Experimental procedure

2.1. Materials and specimen preparation

Tapes have been produced which contain unidirectional E-glass fibre tows and high strength (type II) carbon fibre tows in ratios of 1:0, 4:1, 3:1, 1:1, 1:4 and 0:1, respectively. These tapes were used to prepare model composites containing different ratios (by volume) of carbon fibres to glass fibres, i.e. 0/100, 13/87, 23/77, 37/63, 44/56, 54/46, 64/36, 70/30, 83/17 and 100/0. The properties of the carbon and glass fibres are presented in Table I. An epoxy resin (Ciba–Geigy CY219) with hardener (HY219) in the ratio of 2:1 (by volume) was used as the matrix.

Casting of the model composite systems involved three stages: first, a piece of tape (150 mm × 150 mm) was immersed in a solution of equal volumes of epoxy resin plus hardener, and of acetone. Next, the wetted tape was heated in an oven to 80° C for 15 min to evaporate the acetone. The epoxy resin impregnated tape was gently stretched across a split-frame mould (Fig. 1). Finally, a mixture of epoxy resin and hardener at 100° C was slowly poured into the mould at one end, passing beneath the tape, and displacing air as it slowly filled the mould. The cast plate was then cured at 60° C for 24 h. This technique of impregnating the tape with an epoxy resin/acetone solution followed by casting hot resin around the tape ensured excellent wetting of fibres and reproducibility of each model hybrid composite.

2.2. Specimen design and test method

Rectangular beams tested in three-point bending was the procedure chosen for investigating the fracture energy of hybrid composites. The specimen width varied as determined by the number of carbon fibre and glass fibre tows necessary to give a particular carbon to glass fibre ratio. The arrangement of the fibre tows for each group of specimens is shown schematically in Fig. 2. The thickness of the specimen was determined by considering the following three requirements: (1) the single layer of tape had to be offset from the central plane towards the tensile face so that when each specimen was loaded in flexure all of the fibres were loaded in tension; (2) it was necessary to make a saw cut across the tensile face of the specimen to aid crack initiation; (3) the thickness of the pure epoxy resin layer must be as thin as possible to minimize unstable fracture.

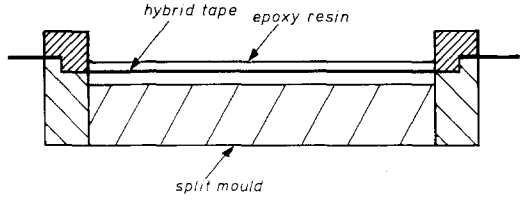

Figure 1 Cross-section of the split frame mould.

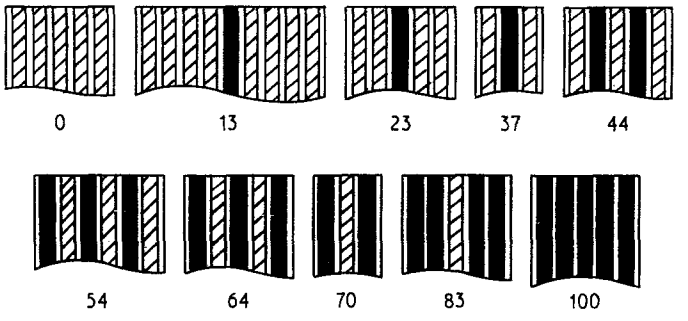

Figure 2 Arrangement of glass fibre tows (hatched) and carbon fibre tows (black) for each specimen group. The numbers beneath each diagram give the percentage (by volume) of carbon fibre in total fibre.

Cooper [13] has shown that in a three-point bend test with width and thickness fixed, the span of the specimen is an important parameter for determining whether failure occurs by stable or unstable cracking. It was found here for the most brittle fibrous composite, carbon fibres in epoxy resin, that spans of 20 mm and 40 mm gave stable and unstable fracture respectively. A length of 20 mm (corresponding to a span to depth ratio of 10:1) was therefore chosen which ensured stable fracture and prevented shear failure. Thus rectangular beams 30 mm long, 2.25 mm thick and 6 to 19 mm wide were machined from the cast plates. Each specimen was tested in three-point bending (Fig. 3) at 18° C (±2° C) at a displacement rate of 2 mm min^{-1} on an Instron testing machine. All of the specimens failed in a controlled manner.

The integral of the load–deflection curve was equated to the total work (U) to break the specimen into two pieces. The work of fracture of the fibrous composite is given by

$$\gamma_F = \frac{U}{2A} \quad (1)$$

where A is the total cross-sectional area of the ends of the fibres in the composite. "Volume fraction" therefore refers to the relative amount of carbon fibres or glass fibres in the total fibre content of the composite, i.e.

$$V_{f(\text{carbon fibre})} + V_{f(\text{glass fibre})} = 1 \quad (2)$$

Any discussion of the fracture energy of these hybrid composites is therefore based on the assumption that the material is essentially a two-phase system where the matrix only serves to bind the fibres together. Work of fracture values calculated in this manner will therefore be higher than those of structural composites where the volume fraction of fibres is of the order of 0.60. A variation in both the volume of fibres in a carbon and glass tow and in the number of carbon fibre and glass fibre tows from one group of specimens to the next, necessitated a normalizing of the work of fracture data with respect to a standard volume of fibre in a specimen containing five carbon fibre tows.

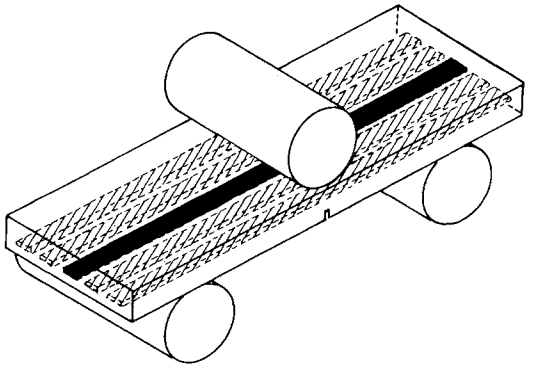

Figure 3 Three-point bending beam specimens.

2.3. Measurement of fibre debonded length and fibre pull-out length

Fibre–matrix debonded zones and the protruding ends of broken fibres can be clearly seen in the model specimens. Pulled out fibres were distinctly visible against a light background when viewed in transmitted light on a Zeiss projection microscope at a magnification of 50 times (Fig. 4b). A tracing was made of each protruding tow by carefully following the dark outline of the pulled out fibre and the fracture surface of the matrix (Fig. 4a). There will be a distribution of fibre pull-out lengths in each tow but the silhouette shows only the longest of these protruding fibres. The maximum average fibre pull-out length, $\bar{l}_{max}$, for each protruding tow was then determined by dividing the area of the tracing by the width of the tow. When the microscope was used in the reflected light mode the fibre debonded zones were clearly visible against a dark background and the average fibre debonded length was

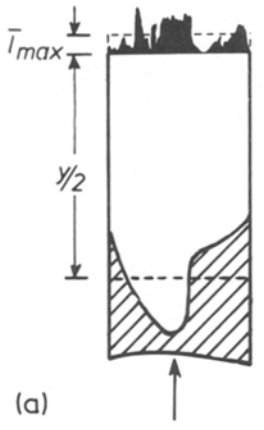

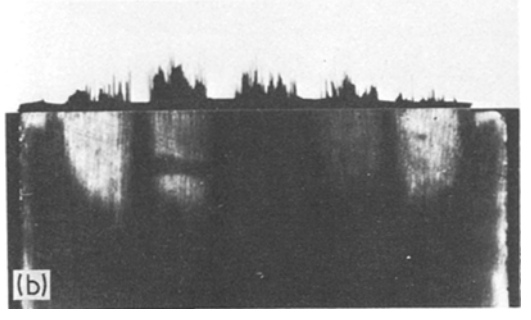

Figure 4 Measurement of the average fibre debonded and pull-out lengths. (a) Tracing of the fibre pull-out and debonded regions for a typical tow in (b). (b) Composite photograph of pull-out and debonded regions viewed in transmitted and reflected light respectively (23% carbon fibre hybrid specimen).

obtained in a similar manner. It was verified, by observation of the opposite face, that the extent of the debonded zones was constant through the thickness of each fibre tow. The maximum average fibre pull-out length and fibre debonded length of each tow in all specimens were measured. Final average fibre debonded lengths and maximum fibre pull-out lengths for each group of model

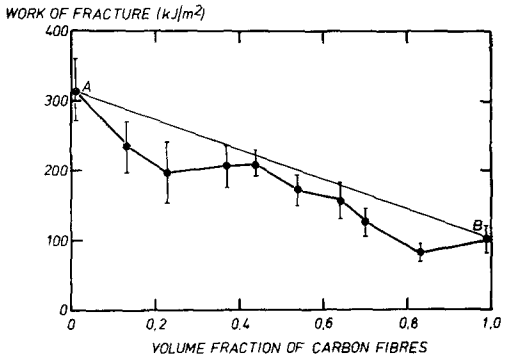

Figure 5 Work of fracture as a function of carbon fibre volume fraction. AB is the rule of mixtures relationship.

composites was found by adding the average values for each tow and dividing by the total number of tows.

3. Results and discussion

The work of fracture data for the hybrid fibrous composites shown in Fig. 5 exhibits a linear relationship with the volume fraction of carbon fibres for volume fractions of between 0.37 and 0.64. These values are still less than predicted by the rule of mixtures equation (Table II);

$$(\gamma_F)_{HYBRID} = (V_f \gamma_F)_{CFRP} + (V_f \gamma_F)_{GRP} \quad (3)$$

There is, however, a pronounced departure from a rule of mixtures prediction for a carbon fibre content of between 13 and 37% and 70 and 90%. A 25% and 40% decrease between the predicted and measured values of work of fracture exists at carbon fibre contents of approximately 23 and 83% respectively. Inhibition and not a synergistic improvement in fracture energy appear to determine the fracture behaviour of carbon fibre/glass fibre/epoxy resin hybrid composites. Fig. 6 is a SEM

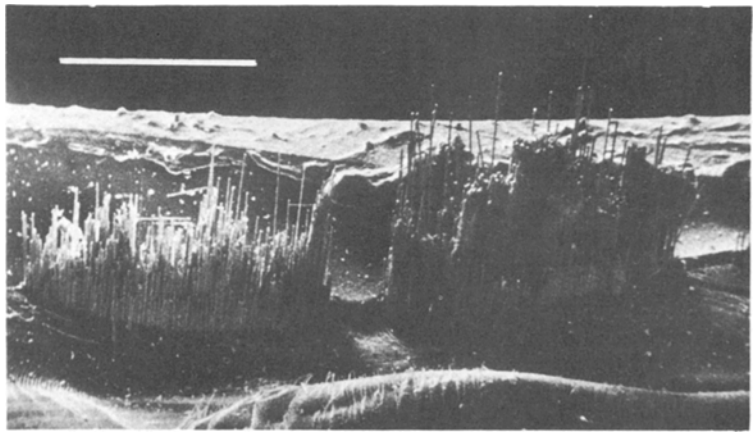

Figure 6 A typical SEM photomicrograph showing the fracture of a carbon fibre tow (left) and a glass fibre tow. (The marker length is equivalent to 1 mm).

TABLE II Experimental results

Carbon fibre volume fraction	No. of specimens	Tape (glass fibre tows/ carbon fibre tows)	Predicted rule of mixtures fracture energy ($kJ\,m^{-2}$)	Normalized work of fracture energy ($kJ\,m^{-2}$)	% Differences	Glass fibre		Carbon fibre	
						Average debonded length, y ($\times 10^{-3}$ m)	Average maximum pull-out length, $\bar{l}_{max}$ ($\times 10^{-3}$ m)	Average maximum pull-out length $\bar{l}_{max}$ ($\times 10^{-3}$ m)	Average debonded length ($\times 10^{-3}$ m)
0.00	5	1:0	–	316 ± 45*	–	5.26	0.46	–	
0.13	4	4:1	288	236 ± 38	−18.1	4.44	0.50	0.64	
0.23	4	4:1	267	197 ± 45	−26.2	4.42	0.44	0.56	
	3	3:1							
0.37	3	4:1	236	205 ± 32	−13.1	4.70	0.46	0.64	< 1
	1	3:1							
	2	1:1							
0.44	7	3:1	221	208 ± 19	− 5.9	5.90	0.54	0.66	
0.54	5	1:1	200	171 ± 22	−14.5	5.28	0.52	0.68	
0.64	6	1:1	178	156 ± 26	−12.4	4.26	0.54	0.62	
0.70	6	1:1	165	125 ± 20	−24.2	3.82	0.56	0.56	
0.83	4	1:4	137	83 ± 8	−39.2	2.34	0.38	0.45	
1.00	5	0:1	–	100 ± 19	–	–	–	0.56	

*Mean ± standard deviation

TABLE III Theoretical models of energy absorption fracture mechanisms

Model	Equation	Reference
Debonding energy	$\gamma_d = \frac{V_f \sigma_f^2 y}{4E}$	[3]
Post debond friction energy	$\gamma_{pdf} = \frac{V_f \tau y^2 \Delta\epsilon}{d}$	[4]
Pull-out energy	$\gamma_p = \frac{V_f \sigma_f l_c}{24}$	[15]

V_f = volume of fractions of carbon or glass fibres in total fibre,
σ_f = ultimate tensile strength of carbon or glass fibres,
l_c = critical transfer length of fibre,
E = Young's modulus of fibre,
y = average debonded length of fibre,
$\Delta\epsilon$ = differential failure strain between fibre and matrix,
τ = interfacial frictional shear stress,
d = fibre diameter.

photomicrograph of a typical fracture surface of a hybrid composite showing the pulled-out carbon fibres and glass fibres. It is viewed from the point of loading and shows a tensile failure of the fibres.

3.1. Analysis of fracture energy

In a model of the fracture of brittle fibrous composites, crack propagation occurs by matrix cracking, shear failure at the fibre–matrix interface, fibres snapping at weak points, fibres retracting in their matrix sockets and by the extraction of broken fibre ends as the two surfaces of a cracked matrix separate. Such fractures processes have been analysed and simple equations derived for their associated energies (Table III). If for carbon fibre/epoxy resin composites, the work of fracture is controlled primarily by the fibre pull-out mechanism [2] while fibre debonding [3, 4], post-debond sliding [4] and fibre pull-out [4, 5] are the major energy absorbing processes in glass fibre/epoxy resin composites, then the total theoretical work of fracture of a fibrous composite containing both carbon fibres and glass fibres may be the sum of these separate energy terms:

$$\gamma_T = (\gamma_p)^c + (\gamma_d)^g + (\gamma_{pdf})^g + (\gamma_p)^g \quad (4)$$

In physical terms, energy is dissipated when a debonded fibre snaps and its stored elastic strain energy is not transferred to the surrounding material but lost as kinetic, acoustic and thermal energies. This results in the retraction of fibre ends in their sockets. An increase in load on the composite causes the broken fibre to slide relative to the matrix over its entire debonded length. The differential displacement between fibre and matrix is assumed in the model to be equal to the product of the fibre debonded length and the difference in failure strains of the fibre and matrix, $y\Delta\epsilon$. Work is done when sliding occurs against friction at the interface. Additional energy may be expended during the extraction of broken fibre ends against a restraining "frictional" shear force when the matrix crack extends.

It is possible to estimate the relative contributions of these four energy terms for the two fibres by using known values of material constants (Table I), measured values of fibre debonded and fibre pull-out lengths (Table II), and by making certain assumptions of the other parameters which we have been unable to measure.

It was assumed that the fibre pull-out length varies linearly through the thickness of each tow between zero and the maximum fibre pull-out length. The average fibre pull-out length $\bar{l}$, is therefore equal to $\bar{l}_{max}/2$ and it is these values which are used in the appropriate energy terms. In the pull-out equation (Table III), the average pull-out length is assumed to be $\bar{l} = l_c/4$ [14], where l_c is the critical fibre length. Using the relationship $\tau/d = \sigma_f/2l_c$ [15] and $\bar{l} = l_c/4$, the post-debond friction energy equation becomes

$$\gamma_{pdf} = \frac{V_f \sigma_f y^2 \Delta\epsilon}{8\bar{l}} \quad (5)$$

It is difficult to be precise about a value for the differential displacement between fibre and matrix, $\Delta\epsilon$, but since the rigidity of the surrounding matrix is relatively high compared to a single fibre and the fact that the resin cracks at very low strains, an estimate for $\Delta\epsilon$ is simply the failure strain of the fibre [4]. If we choose, therefore, a value for $\Delta\epsilon$ of 0.01 for a glass fibre in epoxy resin, then the shape of the theoretical work of fracture γ_T curve matches that of the experimental curve remarkably well.

Examination of the four theoretical energy curves (standard deviations given in Table IV), shows that the debonding energy of the glass fibres and the work to extract broken carbon fibres and glass fibres from the matrix follows a linear relationship with fibre volume fraction, as would be expected from the form of each equation. However, the shape of the theoretical curve for post-debond friction energy is not linear, but is very similar to that of the theoretical work of fracture

TABLE IV Theoretical fracture energies

Carbon fibre volume fraction	Glass fibre debond energy γ_d^g ($kJ\,m^{-2}$)	Glass fibre post debond friction energy γ_{pdf}^g ($kJ\,m^{-2}$)	Glass fibre pull-out energy γ_p^g ($kJ\,m^{-2}$)	Carbon fibre pull-out energy γ_p^c ($kJ\,m^{-2}$)	γ_T ($kJ\,m^{-2}$)
0.00	51.0 ± 2.0*	257.5 ± 42.2	63.3 ± 9.2	–	371.8 ± 35.2
0.13	37.5 ± 1.9	148.6 ± 27.7	58.9 ± 8.9	16.8 ± 1.4	261.8 ± 21.6
0.23	33.0 ± 2.9	146.9 ± 41.8	47.5 ± 9.0	25.5 ± 4.9	252.9 ± 36.3
0.37	29.1 ± 4.2	136.2 ± 46.0	39.3 ± 6.0	47.7 ± 9.8	252.3 ± 57.2
0.44	32.0 ± 4.0	151.0 ± 49.6	42.1 ± 5.9	57.8 ± 11.1	282.9 ± 67.2
0.54	23.4 ± 1.8	105.8 ± 30.9	32.9 ± 5.7	72.8 ± 6.1	234.9 ± 27.5
0.64	14.7 ± 1.8	50.4 ± 13.6	26.9 ± 2.1	78.4 ± 5.7	170.4 ± 16.5
0.70	11.1 ± 2.1	49.0 ± 75.1	23.4 ± 6.6	76.9 ± 8.6	160.4 ± 47.2
0.83	3.9 ± 0.1	10.5 ± 1.9	8.9 ± 1.3	75.5 ± 5.7	98.8 ± 5.9
1.00	–	–	–	110.4 ± 14.2	110.4 ± 14.2

*Mean ± standard deviation.

curve (Fig. 7). These results show that for the model glass-rich hybrid fibrous composites at least, the post-debond friction energy term is a major component of the total work of fracture. For the glass fibre, the fibre debonding energy and fibre pull-out energy terms are comparable in magnitude and the work of fracture of carbon fibre composites can be adequately explained using the fibre pull-out model. The debonded lengths of the carbon fibres were measured and found to be typically less than 1 mm which corresponds to a maximum debonding energy of $6\,kJ\,m^{-2}$ and a post-debond friction energy of $4.8\,kJm^{-2}$ assuming $\Delta\epsilon = 0.014$ (Table I), and were thus not considered to be significant. The work of fracture of the hybrid fibrous composite can therefore be equated to the sum of the following energy terms:

$$(\gamma_F)_{HYBRID} = (\gamma_p)^c + (\gamma_d)^g + (\gamma_{pdf})^g + (\gamma_p)^g \quad (6)$$

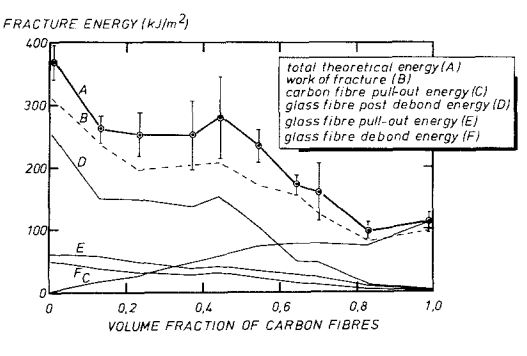

Figure 7 The individual and total theoretical energy terms as a function of carbon fibre volume fraction for the hybrid composite.

Some interaction between carbon fibres and glass fibres is responsible for the variation in the post-debond energy term for glass fibres in the hybrid composite. This term accounts for the unexpected shape of the glass-rich portion of the work of fracture curve. Fibre debonded length is the key parameter in this energy term and the general shape of the work of fracture curve is determined therefore, by the effect of carbon fibres on the glass fibre debonding process. It requires only a 20% (by volume) replacement of glass fibres by carbon fibres for a drop of about 25% in fracture energy with respect to a rule of mixtures prediction. It is of interest to note that at the carbon-rich end of the curve a decrease of about 40% is seen. This is accompanied by a dip in the total theoretical curve, primarily due to shorter carbon fibre pull-out lengths and glass fibre debonded lengths.

4. Conclusions and implications

The use of a model fibrous composite has permitted accurate measurement of fibre debonded length and fibre pull-out length which together with simple models of fracture have enabled a detailed analysis of the mechanisms of cracking in hybrid composites to be undertaken. A negative hybrid effect and a non-linear relationship between work of fracture and fibre composition are due primarily to the effect of the carbon fibres on the post-debond sliding mechanism at the glass fibre/epoxy resin interface. Post-debond friction energy is the dominant term contributing to the fracture energy of glass fibres in epoxy resin, while the fibre debonding energy and fibre pull-out terms

are comparable in magnitude. The dominance of the post debond friction term over the pull-out term for glass fibres is because the debonded lengths are typically 20 times greater than the pull-out lengths. In contrast, the pulling out of broken carbon fibres from a cracked epoxy resin matrix is the principal energy absorbing process for CFRP.

It is important to remember that for structural composites a rule of mixtures relationship between the work of fracture of the hybrids and the CFRP and GRP composites may overestimate the fracture energy of the hybrid composites.

Acknowledgements

The authors would like to thank Mr L. N. Phillips of the Royal Aircraft Establishment, Farnborough, for providing some of the material and for valuable discussions and Mr G. H. K. Rae of Carr Reinforcements, Liverpool, for his help and advice. The continuing assistance of the U. S. Army, contract number DA-ERO-75-G-009, is appreciated. One of us (MM) is grateful to the National Research Council of Canada for its support in the form of a Post-doctoral Fellowship.

References

1. P. W. R. BEAUMONT, *J. Adhesion* **6** (1974) 107.
2. P. W. R. BEAUMONT and B. HARRIS, *J. Mater. Sci.* **7** (1972) 1265.
3. J. O. OUTWATER and M. C. MURPHY, 24th Annual Technical Conference on Reinforced Plastics/Composites Division; Paper 11C (Society of Plastics Industry, Inc., 1969).
4. B. HARRIS, J. MORLEY and D. C. PHILLIPS, *J. Mater. Sci.* **10** (1975) 2050.
5. B. GERSHON and G. MAROM, *ibid.* **10** (1975) 1549.
6. C. C. CHAMIS, M. P. HANSON and T. T. SERAFINI, ASTM STP 497 (1972) 324.
7. B. HARRIS and A. R. BUNSELL, *Composites* **6** (1975) 197.
8. P. W. R. BEAUMONT, P. S. RIEWALD and C. ZWEBEN, ASTM STP 568 (1974) 134.
9. P. G. RIEWALD and C. ZWEBEN, 30th Annual Technical Conference on Reinforced Plastics/ Composites Division (Society of Plastics Industry, Inc., 1975).
10. P. K. MALLICK and L. J. BROUTMAN, *ibid.*
11. D. F. ADAMS and A. K. MILLER, *Mater. Sci. Eng.* **19** (1975) 245.
12. J. L. PERRY and D. F. ADAMS, *Composites* **6** (1975) 166.
13. G. A. COOPER, *J. Mater. Sci.* **12** (1977) 277.
14. B. HARRIS, P. W. R. BEAUMONT and E. MONCUNILL de FERRAN, *ibid.* **10** (1971) 238.
15. A. H. COTTRELL, *Proc. Roy. Soc. (Lond.)* **A282** (1964) 2.

Received 9 December 1977 and accepted 27 February 1978.